CHIN. PHYS. LETT. Vol. 26, No. 7 (2009) 077804

Nondoped Electrophosphorescent Organic Light-Emitting Diodes Based on Platinum Complexes *

YANG Gang(杨刚)[1**], ZHANG Di(张迪)[1], WANG Jun(王军)[1], JIANG Quan(蒋泉)[1], ZHONG Jian(钟建)[1], YU Jun-Sheng(于军胜)[1], ZHU Feng-Zhi(朱凤稚)[1], LUO Kai-Jun(骆开均)[2***], XIE Yun(谢运)[2], XU Ling-Ling(徐玲玲)[2]

[1]*State Key Lab of Electronic Thin Films and Integrated Devices, School of Optoelectronic Information, University of Electronic Science and Technology of China, Chengdu 610054*

[2]*Institute of Chemistry and Materials, Sichuan Normal University, Chengdu 610081*

(Received 15 January 2009)

An undoped electrophosphorescent organic light-emitting diode is fabricated using a pure platinum(Ⅱ) (2-phenylpyridinato-N, C^2) (3-benzoyl-camphor) [(ppy)pt(bcam)] phosphorescent layer acting as the emitting layer. A maximum power efficiency η_p of 6.62 lm/W and current efficiency of 14.78 cd/A at 745 cd/m^2 are obtained from the device. The roll-off percentage of η_p of the pure phosphorescent phosphor layer device is reduced to 5% at a current density of 20 mA/cm^2, which is about 11% for conventional phosphorescent devices. The low roll-off efficiency is attributed to the phosphorescent material, which has the molecular structure of a strong steric hindrance effect.

PACS: 78. 55. −m, 81. 15. Ef, 85. 60. Jb

The performance of organic light-emitting diodes (OLEDs) has improved dramatically in recent years.[1−4] By utilizing phosphorescent dyes, such as platinum and iridum organometallic emitters, the internal quantum efficiency can be, in principle, increased to 100%.[5,6] The organometallic emitters enhance the efficiency of intersystem crossing from the lowest singlet excited state to the lowest lying triplet and thereby enable phosphorescence from the triplet states. Adachi *et al.*[7] reported a maximum external quantum efficiency of 15.4% by doping a green-emitting phosphorescent dye Ir(ppy)$_3$ into an electron transporting host TAZ.

In previous works, the emission layer of the phosphorescent OLED has been fabricated by co-evaporating host materials and phosphorescent dopant. The Dexter energy transfer mechanism is suitable for most phosphor energy transfer processes, in which the energy is transferred from the host material to doped phosphor in the emission layer. The effective current range of Dexter energy transfer is about 10–15 Å, which is shorter than that of Förster energy transfer. Thus the doping concentration of the phosphorescent dye should be higher than that of the fluorescent dye.[8] However, with the doping concentration of the phosphorescent dye increasing, the power efficiency and luminescence of organic device sharply degrade due to triplet-triplet annihilation, electric field induced dissociation of excitons and triplet-polaron annihilation at high driving current density.[9−11] On the other hand, much higher concentrations of the phosphorescent dye could be recrystallized, which results in a non-radiation phenomenon in phosphor doped devices. The complicated doping process and the quick device efficiency roll-off under high current density are two key problems, which are not propitious for further expansion of the doping phosphor device.

Recently, an ultrathin layer instead of doping structure has been reported in some OLEDs in order to decrease the difficulty of adjusting co-evaporating organic materials and to improve the stability and reproducibility of OLEDs.[12−14] Conventionally, the thickness of the ultrathin emitting layer is not greater than 6nm. According to the evaporating film theory, the deposition thickness must be thicker than 10nm in order to form a continuous film, which is deposited by vacuum thermal evaporation. It should be noticed that a deposition-film thickness lower than 10nm would not be an exactly continuous film. Herein, this structure of the ultrathin emitting layer OLEDs is not that of real nondoped devices. A pure phosphor emitting layer structure is seldom reported.

In this Letter, we demonstrate a phosphorescent OLED with pure phosphorescent materials as the emitting layer based on the materials [(ppy)pt(bcam)] with red light emission. Because the molecular structure of this kind of phosphorescent material has a 3-benzoyl-camphor group with a strong steric hindrance effect, this group can effectively prevent (ppy)pt(bcam) phosphorescent molecules from aggregating. Therefore, the concentration quenching effect is not observed in the pure (ppy)pt(bcam) layer phosphorescent device. At the same time, a pure phosphor layer instead of doping structure in PhOLEDs can remarkably reduce power efficiency roll-off at high current density in the devices, which means that the device shows the performance of long-lifetime stabil-

*Supported by the National Natural Science Foundation of China under Grant No 20472060.

**Email: uestcyanggang@yahoo.com.cn

***Email: luo-k-j007@163.com

© 2009 Chinese Physical Society and IOP Publishing Ltd

ity. The reason that causes the efficiency to decrease slowly with this nondoped phosphor layer structure is also shown in the following experiments.

Indium tin oxide (ITO)-coated substrate with a sheet resistance of about 15 Ω/square was ultrasonically cleaned with detergent water, water, deionized water, ethanol and acetone 20 min in each step. Prior to organic layer deposition, the dried ITO-coated substrate was treated by oxygen plasma for 2 min and then loaded into an organic vacuum evaporation chamber with a pressure of 10^{-7} Torr by robot. The multilayer organic films were subsequently deposited at a rate of 0.3–1 Å/s without breaking the vacuum. Then the substrate with organic layers was transported to a metal evaporation chamber with robotic assistance to evaporate a 1-nm lithium fluoride (LiF) layer and 100 nm aluminum (Al) cathode. The device structure is ITO/4,4′,4″-tris[*N*-(2-naphthyl)-*N*-phenyl-amino] triphenylamine (2TNATA)(30 nm)/*N*, *N*′-bis(naphthalen-1-yl)-*N*, *N*′-bis(phenyl)-benzidine (NPB) (40 nm)/(ppy)pt(bcam) (*x* nm)/2, 9-dimethyl-4, 7-diphenyl-1.10-Phenanthroline (BCP) (20 nm)/tris(8-hydroxyquinoline) aluminum (Alq) (20 nm)/LiF (1 nm)/Al (100 nm) ($x = 10$ nm for device A and $x = 20$ nm for device B), device C with a structure of ITO/2TNATA(30 nm)/NPB(40 nm)/4,4′-N,*N*′-dicarbazole-biphenyl (CBP): (ppy)pt(bcam) (9 wt%, 20 nm)/BCP (20 nm)/Alq (20 nm)/LiF (1 nm)/Al (100 nm), and device D with a structure of ITO/2TNATA(30 nm)/NPB(40 nm)/CBP: [fac-Tris (2-phenylpyridin)-iridium] ($Ir(ppy)_3$(9 wt%, 30 nm)/BCP (20 nm)/Alq (20 nm)/LiF (1 nm)/Al (100 nm). ITO and LiF/Al were used as anode and cathode, respectively. 2TNATA, NPB, BCP and Alq are used as hole injection layer (HIL), hole transport layer (HTL), hole blocking layer (HBL) and electron transport layer (ETL), respectively. CBP was used as the host material. Device C was fabricated for comparison on power efficiency characteristics between the nondoped PhOLED and the doped PhOLED. The nondoped device structure and all the materials used are shown in Fig. 1.

The layer thickness and deposition rate of organic and inorganic materials were monitored *in situ* by oscillating quartz thickness monitors. EL spectra and Commission International de l'Eclairage (CIE) (1931) coordinates of the devices were measured with a PR650 spectroscan spectrometer. Characteristics of the luminance L, current density J, bias voltage V were recorded simultaneously with the measurement of EL spectra by combining the spectrometer with a Keithley 2400 programmable voltage-current source. All the measurements were performed at room temperature in ambient conditions.

Figure 2 illustrates the $J - V - L$ characteristics of devices A and B. It shows that the luminance of devices A and B are 8359 cd/m^2 and 5185 cd/m^2 at 14 V, respectively, and the turn-on voltage (defined as the bias at $L = 1$ cd/m^2) of both the devices is about 5.0 V. The current densities of these devices increase with the forward bias, but there is little difference between J values at low voltage regions. Device A with a phosphorescent thinner layer shows higher J than that of device B. The inner resistance of the device decreases as the thickness of phosphorescent emitting layer is reduced. As is well known, the highest occupied molecular orbital (HOMO) level of NPB is 5.5 eV, i.e. 0.4 eV lower than that of (ppy)pt(bcam). In contrast, the lowest unoccupied molecular orbital (LUMO) level of NPB is 2.3 eV, i.e. 0.5 eV higher than that of phosphor. An electron trap and a hole trap will be formed in the phosphor emitting layer. The carrier traps can significantly capture the electrons from BCP (HBL) and the holes from NPB (HTL).

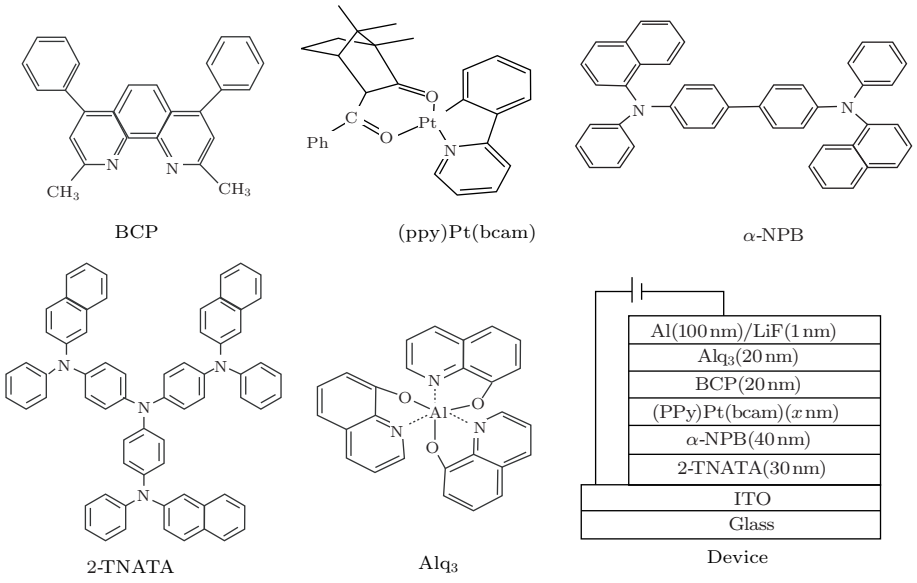


Fig. 1. Molecular structure of the materials used and the nondoped device configuration.

Hereby the current density of device A is higher than device B at low voltage. However, some holes will hop to the HOMO of the phosphor layer under forward electronic field and then combine with electrons at the interface between NPB and BCP. As the voltage increases, the limited function of the 0.4 eV barrier at the interface between the phosphor layer and the NPB layer becomes weaker under high electronic field, and the current densities of both devices become equivalent, as shown in Fig. 2.

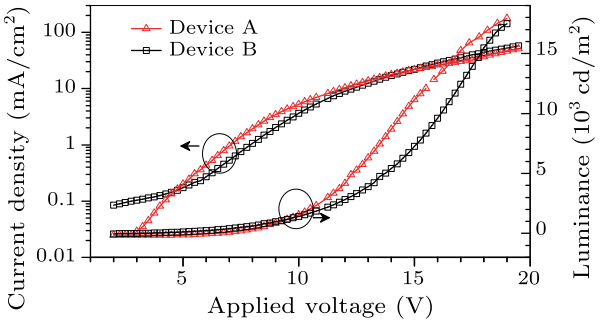


Fig. 2. $J-V-L$ characteristics of devices A and B.

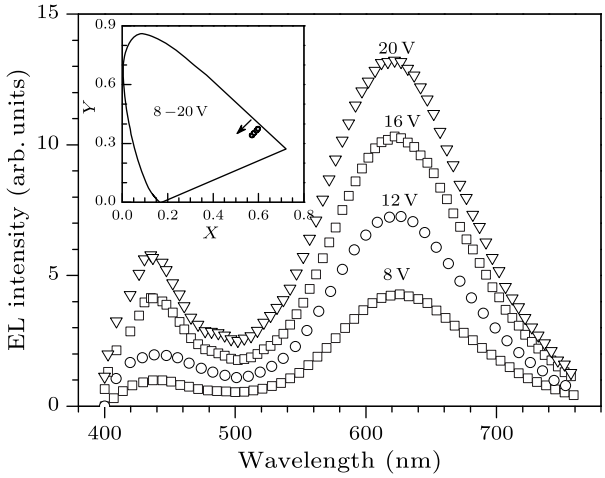


Fig. 3. Normalized EL spectra of device A at forward bias values of 8, 12, 16, 20 V. Inset: the CIE coordinates of the device.

There are two emission peaks in the normalized EL spectra of device A, as shown in Fig. 3. The peak at 625 nm is the emission spectrum of (ppy)pt(bcam), and its emission intensity increases with increasing forward bias. However, the main peak of the emission spectrum of (ppy)pt(bcam) almost has no change. It is obvious that the electro-phosphorescent characteristics of (ppy)pt(bcam) are very stable. Actually, the emission spectrum characteristics of device B have nearly the same trend as that of device A. A weak peak at 429 nm from NPB was found in the EL spectra of device A. The density ratio of the NPB peak at 429 nm to the (ppy)pt(bcam) peak at 625 nm is about 1:8 at a forward bias of 8 V. The EL spectra indicate that the relative emission intensity of the peak at 429 nm from NPB increases more quickly than that of (ppy)pt(bcam) with voltage enhancement. Stable red light is emitted from the two devices at different voltages, and the Commission Internationale de l'Eclairage (CIE) coordinates of devices A are (0.633, 0.376) at 12 V and (0.608, 0.358) at 20 V, respectively, as shown in the inset of Fig. 3. The CIE coordinate shift of device A with voltage enhancement is attributed to the change of the relative emission intensity of NPB to (ppy)pt(bcam). In most white-light-emitting OLEDs, the intensity ratio of blue light will be promoted with voltage enhancement. Especially in direct trapping devices, higher electronic field intensity reduces the trapping actions of phosphor and promotes the emission of high energy level exciton material such as NPB.[15]

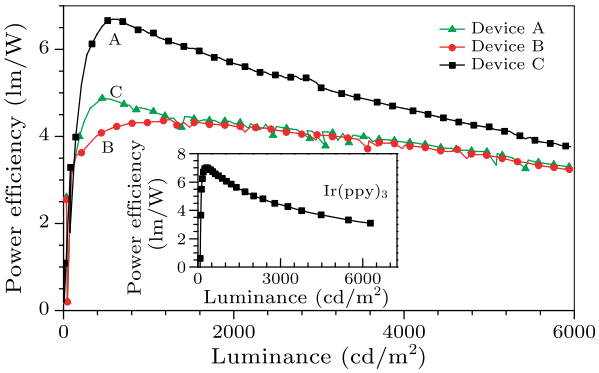


Fig. 4. Power efficiency η_p of devices A, B and C vs luminance. Inset: η_p of device D with the conventional structure.

The power efficiency η_p of devices A, B and C versus luminance are shown in Fig. 4, for comparison, η_p of device D with conventional structure is also provided in the inset. With the increase of bias, the η_p values of the three devices are improved at low voltage, and then slowly decrease at high current density. The characteristics of η_p, current efficiency η_l, and the efficiency roll-off of the four devices are listed in Table 1. A maximum η_p of 6.62 lm/W at $L = 745$ cd/m^2 can be obtained for device A, a maximum η_p of 4.08 lm/W at $L = 1022$ cd/m^2 for device B, and a maximum η_p of 4.67 lm/W at $L = 976$ cd/m^2 for device C. There is very little difference between the characteristics of η_p of device B and device C. It is certified that the strong steric hindrance effect group can effectively prevent the (ppy)pt(bcam) molecules from aggregating. However, the luminance of device D at maximum η_p(8.18 lm/W) is only 38 cd/m^2, which is not very suitable for practical applications. On the other hand, the power efficiency drops to 33.5% of the maximum η_p when $L = 5000$ cd/m^2. Nevertheless, for device A, the power efficiency only reduces to 78.8% (η_p/η_p maximum) at $L = 5000$ cd/m^2, to 85.7% and 82.1% for devices B and C, respectively. It is indicated that the roll-off of power efficiency is significantly weakened by the (ppy)pt(bcam) phosphor layer with the group strong steric hindrance effect.

Table 1. Power efficiency, luminance efficiency, and roll-off characteristics of the three PhOLEDs.

Device code	η_p(max) (lm/W) at L(cd/m^2)	η_l(max) (cd/A) at L (cd/m^2)	η_p ($L = 5000$ cd/m^2)/η_p (max)	η_p($J = 20$ mA/cm^2)/η_p(max)
A	6.62 at 745	15.60 at 480	0.79	0.95
B	4.08 at 1022	10.63 at 2237	0.86	0.98
C	4.67 at 976	11.78 at 1516	0.82	0.97
D	8.18 at 38	20.63 at 350	0.33	0.53

In most PhOLEDs, excitons are formed at the interface of the emission layer and HBL, which is due to higher hole mobility than electron mobility in the emissive layer and easy hole injecting from anode to organic material. As device current density increases, the combined area of free carriers will shift and become wider, so the recombination processes start to dramatically affect device efficiency.[4,16] Restricting the light emission region is an effective method to reduce the rapid dropping of device efficiency at large current densities. Free carriers injected into the emission layer can be directly trapped by (ppy)pt(bcam) molecules due to the energy level barrier with adjacent materials and combine to form orange to red light emission on phosphors in two devices.

In summary, high efficiency red light PhOLEDs have been fabricated with a pure phosphorescent material (ppy)pt(bcam) emission layer structure. The devices show a maximum power efficiency of 6.62 lm/W at 745 cd/m^2, 4.08 lm/W at $L = 1022$ cd/m^2 and a maximum current efficiency of 15.60 cd/A at 480 cd/m^2, 10.63 cd/A at 2237 cd/m^2, for devices A and B, respectively. The power efficiency of the devices at $J = 20$ mA/cm^2 dropped to 95.2% and 97.9% of the maximum value for devices A and B, respectively. For comparison, we also fabricated a doped device, C, whose relative characteristics are almost the same as those of device B. It is indicated that the low roll-off power efficiency of PhOLEDs at high current density could be realized by the stable phosphorescent material (ppy)pt(bcam) with a strong steric hindrance effect.

References

[1] Baldo M A, O'Brien D F, You Y, Shoustikov A, Sibley S, Thompson M E and Forrest S R 1998 *Nature* **395** 151
[2] Sun Y, Giebink N C, Kanno H, Ma B, Thompson M E and Forrest S R 2006 *Nature* **440** 908
[3] Gong X, Ostrowski J C, Moses D, Bazan G C and Heeger A J 2003 *Adv. Funct. Mater.* **13** 439
[4] Yu J, Li W, Jiang Y and Li L 2007 *Jpn. J. Appl. Phys.* **46** L31
[5] Adachi C, Baldo M A, Thompson M E and Forrest S R 2001 *J. Appl. Phys.* **90** 5048
[6] Ikai M, Tokito S, Sakamoto Y, Suzuki T and Taga Y 2001 *Appl. Phys. Lett.* **79** 156
[7] Adachi C, Baldo M A, Forrest S R and Thompson M E 2000 *Appl. Phys. Lett.* **77** 904
[8] Klessinger M and Michl J 1995 *Excited States and Photochemistry of Organic Molecules* (New York: VCH) p 290
[9] Baldo M A, Adachi C and Forrest S R 2000 *Phys. Rev.* B **62** 10967
[10] Reineke S, Walzer K and Leo K 2007 *Phys. Rev.* B **75** 125328
[11] Kalinowski J, Stampor W, Mezyk J, Cocchi M, Virgili D, Fattori V and Marco P D 2002 *Phys. Rev.* B **66** 235321
[12] Jiang X, Zhang Z, Zhu W and Xu S 2005 *J. Phys.* D **38** 4153
[13] Choukri H, Fischer A, Forget S, Chénais S, Castex M, Adès D, Siove A and Geffroy B 2006 *Appl. Phys. Lett.* **89** 183513
[14] Tsuji T, Naka S, Okada H and Onnagawa H 2002 *Appl. Phys. Lett.* **81** 3329
[15] Wang J, Yu J S, Li L, Wang T, Yuan K and Jiang Y D 2008 *Appl. Phys. Lett.* **92** 133308
[16] Kang J, Lee S, Park H, Jeong W, Yoo K, Park Y and Kim J 2007 *Appl. Phys. Lett.* **90** 223508